Pergamon

Tetrahedron, Vol. 52, No. 46, pp. 14419-14436, 1996

0040-4020/96 $15.00 + 0.00

PII: S0040-4020(96)00875-7

SYNTHESIS, BIOPHYSICAL PROPERTIES, AND STABILITY STUDIES OF MIXED BACKBONE OLIGONUCLEOTIDES CONTAINING SEGMENTS OF METHYLPHOSPHOTRIESTER INTERNUCLEOTIDIC LINKAGES

Radhakrishnan P. Iyer, Dong Yu, Zhiwei Jiang and Sudhir Agrawal

Hybridon Inc., One Innovation Drive, Worcester, MA 01605, USA

Abstract: The synthesis of mixed-backbone-oligonucleotides (MBOs) (15 to 25-mers) which contain phosphoric diester (PO) or phosphorothioate (PS) backbones along with segments of internucleotidic *O*-methylphosphate (POOMe) or *O*-methylphosphorothioate (PSOMe) linkages have been accomplished using *N*-pent-4-enoyl (*PNT*) nucleoside phosphoramidite synthons. The T_ms of the MBOs reveal that they form stable duplexes with complementary DNA and RNA. The MBOs also showed increased resistance to degradation by nucleases. Consequently, the MBOs with methylphosphotriester segments represent a novel class of antisense oligonucleotides with potential for therapeutic and diagnostic applications. Copyright © 1996 Elsevier Science Ltd

INTRODUCTION

Oligonucleotides which contain internucleotidic phosphotriester linkages[1] have served as very useful probes in the study of nucleic acid-protein interactions.[2] Being small in size and non-ionic, the substitution of O^- in a phosphoric diester backbone by OMe group is expected to produce only minimal steric perturbation in a modified oligonucleotide, an important attribute in helping to decipher the nature of the interaction between the backbone and the interacting partner.[1]

The rapidly evolving field of nucleic acid therapeutics[3] has rekindled interest in these novel molecules particularly as potential antisense agents. In this regard, phosphorothioates and, to a lesser extent, the non-ionic methylphosphonate oligonucleotides have occupied the center stage as antisense agents. However, from a pharmacokinetic and pharmacodynamic perspective,[4] it is anticipated that a mixed backbone oligonucleotide (MBO), which incorporates both ionic and non-ionic segments, in a modular oligonucleotide design, would be advantageous (Figure 1). For example, in an *in vivo* situation, an MBO is expected to have these additional attributes compared to phosphorothioates: (a) longer plasma half-life, (b) lesser backbone-related unproductive interactions with cellular macromolecules, and decreased polyanion-mediated side effects, (c) increased cellular uptake, (d) enhanced resistance against nucleases, and (e) formation of discrete degradation fragments resulting from metabolism of the MBO which would be rapidly cleared by excretion. Furthermore, although it is generally recognized that the duplex of a non-ionic oligonucleotide with complementary RNA is not a substrate for RNase H, that of an MBO containing non-ionic segments, in conjunction with phosphoric diester (PO), or phosphorothioate (PS) backbone segment is known to be a substrate for RNase H.[5a,b] From a therapeutic

perspective, oligonucleotides which activate RNase H towards cleavage of the RNA strand are expected to show

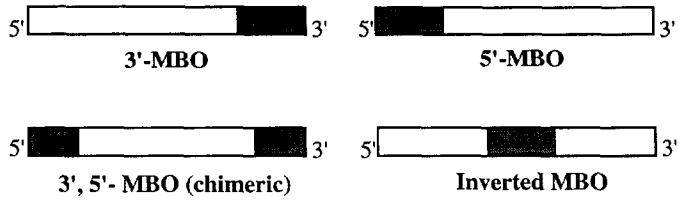

Fig. 1. Examples of mixed backbone oligonucleotide (MBO) designs; The shaded area represents the non-ionic segments, while the unshaded area represents the ionic segments.

improved antisense activity because of their potential for catalytic effect. Thus, by harnessing the benefits of both ionic and non-ionic type oligonucleotides, an MBO is expected to have better bioavailability, lesser side effects, and enhanced overall potential for therapeutic applications.

Being small in size and non-ionic, the presence of methylphosphotriester groups in an MBO, could potentially allow for stronger hybridization with its complementary partner because of decreased phosphate to phosphate charge repulsion between their backbones. In fact, molecular mechanics calculations have revealed that methylphosphotriester duplexes preferentially adopt a B DNA conformation irrespective of the configurations of the P-chiral centers because both the R_p and S_p methylphosphotriester groups are perfectly accommodated within the B DNA double helix.[6] This is in contrast to other P-chiral non-ionic oligonucleotides such as methylphosphonates, wherein significant differences in the hybridization characteristics of the individual stereoisomers have been reported.[7]

With these objectives in mind, we have examined MBOs with methylphosphotriester type non-ionic linkages. We have recently reported the use of *N*-pent-4-enoyl (*PNT*) nucleosides in the preparation methylphosphotriester oligonucleotides.[8a,b] Herein, we describe the synthesis, biophysical characteristics, stability studies and selected biological properties of MBOs which incorporate methylphosphotriester linkages at defined positions within a phosphoric diester or phosphorothioate oligodeoxynucleoside framework.

RESULTS AND DISCUSSION

Synthesis of oligonucleotides using PNT phosphoramidites; Evidence for fidelity of synthesis

Before embarking on the synthesis of MBOs of longer length, it was important to establish that the deprotection protocols employed would ensure complete nucleobase and phosphate deprotection without any attendant nucleobase modifications. Towards this objective, a 15-mer phosphoric diester oligonucleotide GGT GGT GGT GGT GGT was prepared[8c] with PNT nucleoside-β-cyanoethyl phosphoramidite (*CEPNT*) synthons using standard solid-phase phosphoramidite chemistry except that during the synthesis cycle, *tert*-butyl hydroperoxide was used for the oxidation of the internucleotidic phosphite linkages. The CPG was divided into two portions and independently subjected to deprotection protocols using either: (a) iodine (2% *w/v*) in pyridine/methanol, 98/2 (30 min, rt) followed by K_2CO_3/MeOH (0.05 M, 24 h, rt) *or*, (b) prolonged exposure to

K_2CO_3/MeOH (0.05 M, 30-36 h, rt). In each case, the oligonucleotide was isolated and purified by standard protocols and subjected to base composition analysis. Figure 2 (Panels A and B) shows the HPLC profiles of the enzyme digests of samples prepared by the two deprotection protocols. As is clearly seen in Figure 2,

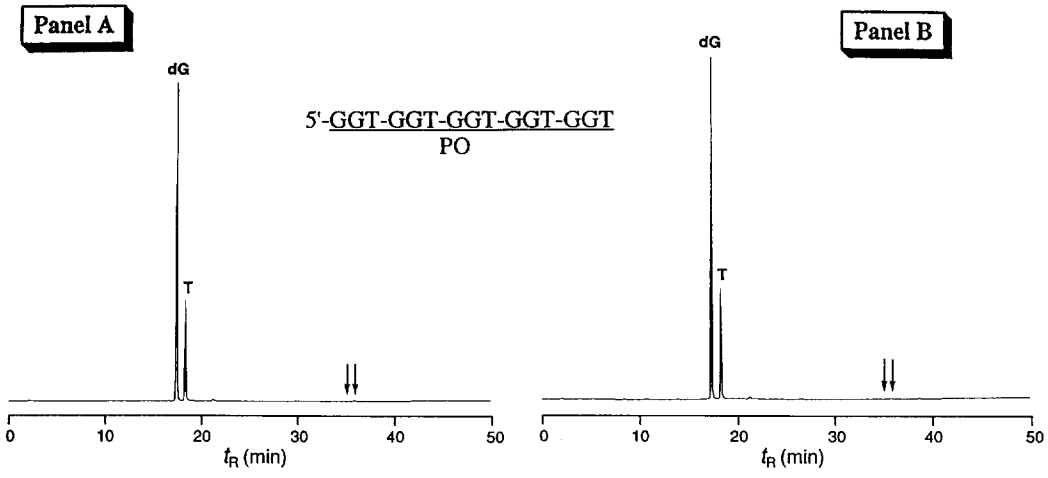

Fig. 2. Reversed-phase HPLC profiles of *SVPD* and *alkaline phosphatase* digests of PO oligonucleotide 5'd[GGT-GGT-GGT-GGT-GGT] prepared using deprotection protocols *either* I_2/pyr/MeOH followed by K_2CO_3/MeOH (**Panel A**) *or* alternatively, extended treatment with K_2CO_3/MeOH (**Panel B**). Arrows indicate the expected positions of dG^{PNT} and the addition product[8c]

complete phosphate and base deprotection had been achieved using either protocols without any attendant base modifications. Furthermore, MALDI-TOF mass spectrum (Figure 3) of the oligonucleotide revealed a molecular ion at 4750.89 (calcd mol. wt. 4751.135). The MALDI-TOF mass spectrum was characterized by the presence of mass ions at 4600.98 and 4451.72 which probably represents laser-induced depurination (removal of guanine residues) of the molecular ion. Additionally, the peak at 2374.2 represents the doubly ionized species which migrated at an apparent molecular weight of 1/2 of the parent ion at 4751.2. The peak at 900.092 corresponds to the $d[GGT]^+$ ion.

These results demonstrated that the above deprotection and cleavage protocols, if employed in the case of MBOs with either POOMe or PSOMe linkages (*vide infra*), would ensure: (a) nucleobase deprotection, (b) decyanoethylation of the phosphate group, (c) cleavage of the oligonucleotide from the support and, (d) optimal recovery of the oligonucleotide.

Synthesis and structure elucidation of MBOs

The facile synthesis of tri- and nonanucleotide MBOs containing methylphosphotriester linkages have been previously described.[8a,b] Using our synthetic strategy, both *O*-methylphosphate (POOMe) and *O*-

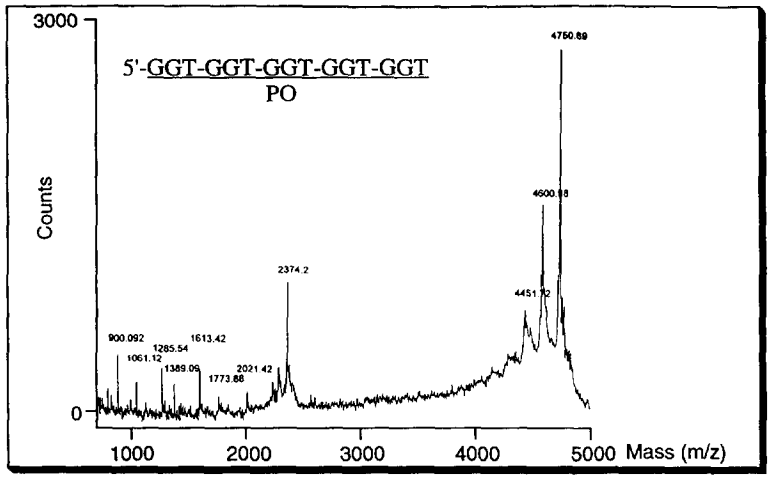

Fig. 3. MALDI-TOF mass spectrum of 5'd[GGT-GGT-GGT-GGT-GGT] prepared using CEPNT amidites.

methylphosphorothioate (PSOMe) linkages can be incorporated in an MBO. For the present study, the MBOs of longer length (15 to 25-mers) were required. Prompted by earlier reports[1,9] and our own experience regarding the base-labile nature of the phosphotriester linkages, careful evaluation of the synthesis and deprotection protocols was necessary to ensure that the methylphosphotriester linkages were intact particularly in MBOs of longer length (15- to 25-mers) wherein prolonged exposure to deprotection reagents was necessary .

In an initial model study designed to ascertain the structural integrity of the methylphosphotriester group, we prepared the MBOs **1** and **2**. Scheme 1 illustrates the synthesis of **1** and **2** using phosphoramidite chemistry[10] on controlled-pore-glass (CPG) supports. In each case, the PO/PS segment was assembled using the β-cyanoethyl (*CEPNT*)- and the POOMe/PSOMe segment using methoxy (*MEPNT*)-nucleoside phosphoramidite synthons respectively.[8a,b] The installation of the POOMe linkages was accomplished by using *tert*-butyl hydroperoxide (1 M in toluene) as the oxidant whereas the incorporation of PSOMe linkages was done using 3*H*-benzodithiole-3-one-1,1-dioxide.[11] The removal of the *PNT* groups from the nucleobases, of the β-cyanoethyl phosphate protecting group, and the cleavage of the oligonucleotide from the support were accomplished by following either of these two protocols: (a) iodine/pyridine/methanol followed by exposure to K_2CO_3/MeOH (0.05 M, rt, 24 h) (protocol A) or (b) prolonged exposure to K_2CO_3/MeOH (0.05 M, rt, 30 to 36 h) (protocol B). Surprisingly, our initial attempts to characterize the MBOs (prepared using both protocols A, and B) by analytical PAGE (using sequencing gel apparatus), in conjunction with UV shadowing, was complicated by the appearance of rather broad bands instead of sharp bands that are normally seen with PO and PS oligonucleotides. The appearance of the broad bands was disconcerting, because it could imply the potential presence of products resulting from varying degrees of demethylation of the phosphotriester linkages during synthesis and deprotection. That this was not the case became apparent only after a systematic evaluation of each step during synthesis, deprotection and analysis conditions. Interestingly, we found that the methylphosphotriester linkages were degraded by TRIS-borate buffer, the running buffer employed during PAGE, at temperatures of 45 to 55 °C. Indications to this phenomenon became clear in a model study in which we found that a PSOMe dinucleoside when heated in the presence of TRIS-borate buffer (0.09 M each in Tris

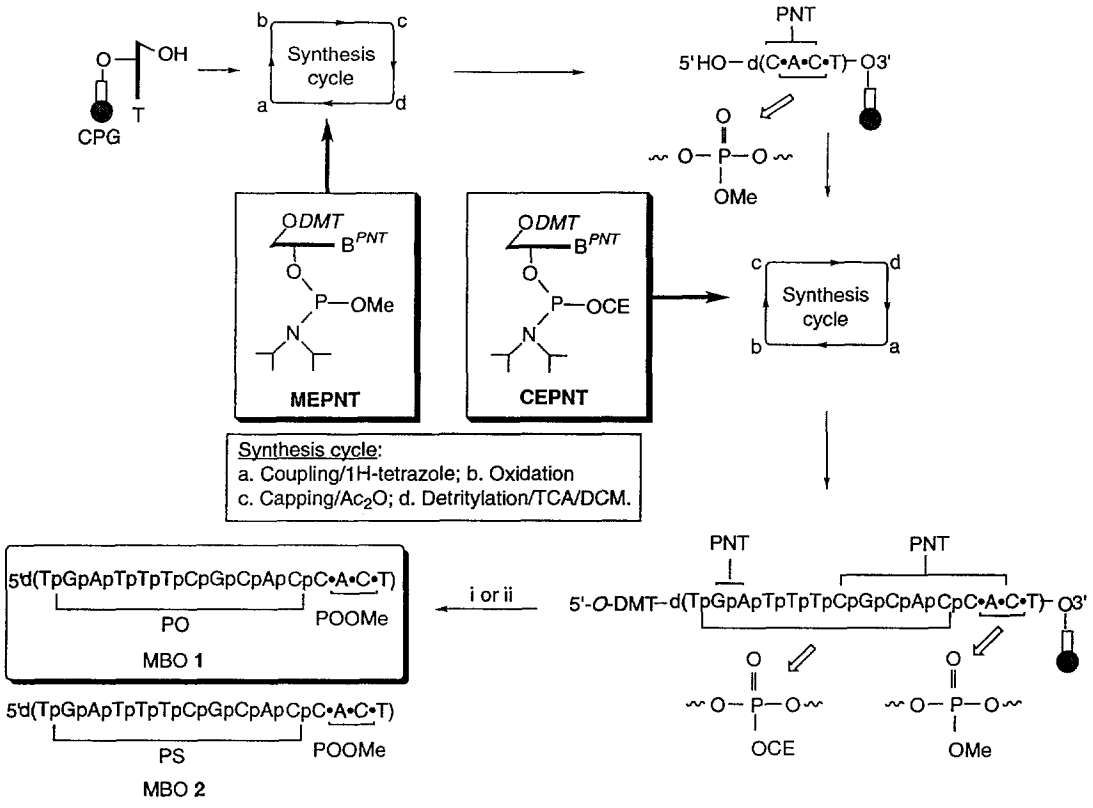

Scheme 1. Typical synthesis of an MBO 1: (i) Deprotection using protocol A , I_2 (2% in pyridine/MeOH, 98/2) followed by K_2CO_3/MeOH (0.05 M, rt, 24 h); (ii) Deprotection using protocol B, K_2CO_3/MeOH (0.05 M, rt, 30 to 36 h)

and boric acid) (55 °C, 4 h) suffered decomposition (10-20%) to yield the corresponding demethylated products (evaluated by reversed-phase HPLC). However, the dinucleoside triester was quite stable when exposed to this buffer at room temperature. Following upon these observations, when the PAGE analysis of **1** and **2** was done in an assembly equipped for water circulation, sharper bands were seen when examined by the UV shadowing technique. Thus, all subsequent PAGE of the MBOs was done using the assembly equipped with a water-circulating system.

In studies designed to ascertain the structural integrity of the methylphosphotriester group, the synthesis, isolation, and structure elucidation of representative MBOs **3** and **4** which have both PO and POOMe linkages were undertaken. The oligonucleotides were isolated by preparative polyacrylamide gel electrophoresis (PAGE) (run at 15-25 °C), and subjected to enzymatic digestion with *snake venom phosphodiesterase* and *bacterial alkaline phosphatase*. Figure 4 shows the digestion profiles of **3** and **4**. In the case of **3**, (Figure 4, Panel A),

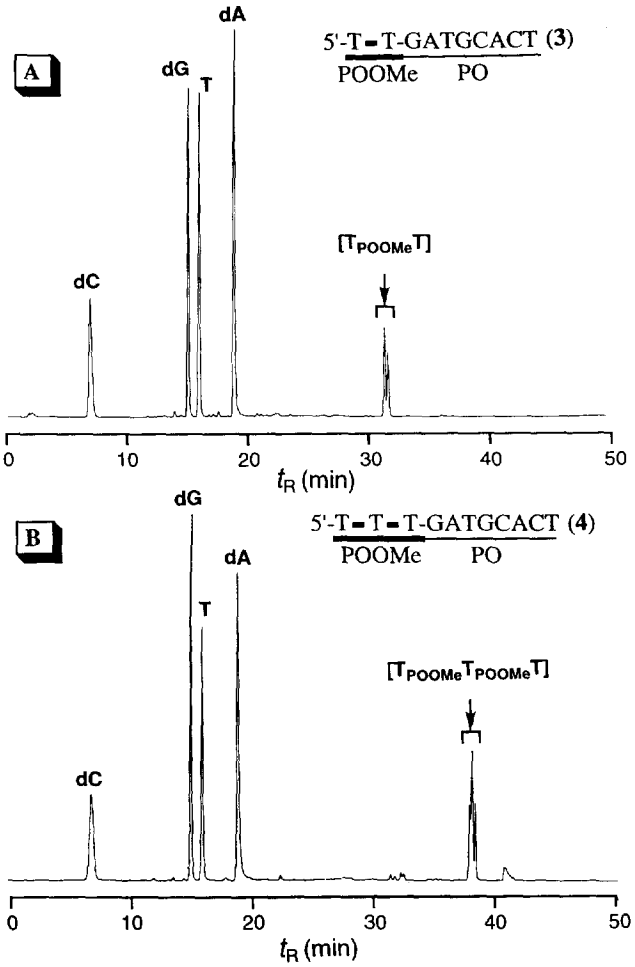

Fig. 4. Reversed-phase HPLC profiles of *SVPD* and *alkaline phosphatase* digests of MBOs **3** and **4**.

the presence of deoxyadenosine (dA), deoxyguanosine (dG), deoxycytidine(dC) and thymidine (T) and the two diastereomers of POOMe dinucleoside [$T_{POOMe}T$], in the expected ratio, was clearly evident. Again, in the case of the MBO **4**, (Figure 4, Panel B), the free nucleosides (dA, dC, dG and T) were found in the expected integral ratio along with the presence of trinucleoside triester [$T_{POOMe}T_{POOMe}T$] fragment.

In order to ascertain that there was no significant amounts of demethylated products in the MBO, we synthesized an MBO **4a** which has a single dinucleoside triester $T_{POOMe}T$ segment at the 5'-end. The oligonucleotide was subjected to enzymatic digestion and analyzed by HPLC as before. As revealed in Figure 5, the $T_{POOMe}T$ linkage was present to the extent of 97% and presence of the TT diester resulting from demethylation during purification and isolation was minimal (< 3%). Incidentally, the use of ^{31}P NMR for structure verification of **3**, **4** and **4a** was less diagnostic, because both the PO as well as POOMe signals appeared at ca δ -0 to -1 ppm with significant overlap of the signals.

The MBOs **5-7** which incorporate one, two, and three PSOMe internucleotidic linkages respectively at the 5'-end, in a phosphorothioate framework, were also prepared and isolated by preparative PAGE (run at 15-25 °C). Figure 6 shows the ^{31}P NMR profiles (Panel A) of PAGE-purified **5-7** and their analytical PAGE (run at 15-25 °C) (Panel B). In PAGE, the mobility of **5-7** was slower compared to the parent "all PO" analog **8** or the "all PS" analog **9**. In the ^{31}P NMR, the expected integral ratio of the PSOMe segment/PS segment was observed in each case.

Taken together, these experiments were suggestive that: (a) the bases were completely deprotected, (b) there was no nucleobase modification when the *PNT* nucleosides were employed in oligonucleotide synthesis, (c) The phosphotriester linkage was reasonably stable to the synthesis reagents (employed in standard solid-phase phosphoramidite methodology), deprotection, as well as processing conditions, and (d) the internucleotidic phosphotriester linkages were resistant to nuclease-mediated degradation. Additionally our results suggest that demethylated products, if present in the MBOs, following purification and isolation, would be less than 5% which is perfectly acceptable for antisense applications of MBOs.

Biophysical properties of MBOs

Having established reliable synthesis, deprotection and analysis procedures, the stage was set to systematically evaluate the influence of the methylphosphotriester linkage on the biophysical and biochemical properties of MBOs. In this context, it is pertinent to mention that, with very few exceptions, the incorporation of novel non-ionic backbone segments (specifically the dephospho-internucleosidic linkages) in an oligonucleotide seems to adversely affect the hybridization characteristics as reflected in a reduction in the T_m of their duplexes with a complementary partner.[3b] In many instances, a reduction in the T_m of 2 to 3 °C per modification has been observed.[12] The factors which contribute to this drop in T_m and the consequent destabilization of the duplex are not fully understood but may involve: (a) a change in the "sugar pucker" introduced by the presence of the modified internucleotidic linkage, (b) the loss of cation-binding sites on the phosphate backbone and the consequent decrease in the duplex-stabilizing interactions, and (c) steric constraints imposed by the P-substituents which might "skew" the normal phosphate geometry in the duplex.

In the event, we prepared the analogs **10-22** (Table 1) which encompass the MBO designs shown in Figure 1. These analogs incorporate both POOMe and PSOMe linkages as the non-ionic core within a PS or PO framework. For comparison, the "all PO" (**23**) and the "all PS" (**24**) oligonucleotides were also prepared.

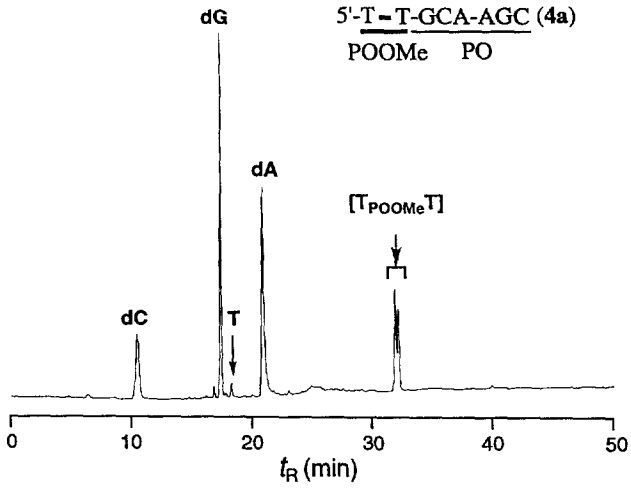

Fig. 5. Reversed-phase HPLC profiles of *SVPD* and *alkaline phosphatase* digests of MBO **4a.** The small peak (3%) at ca. 18 min presumably corresponds to T nucleoside resulting from enzymatic digestion of demethylated $T_{POOMe}T$.

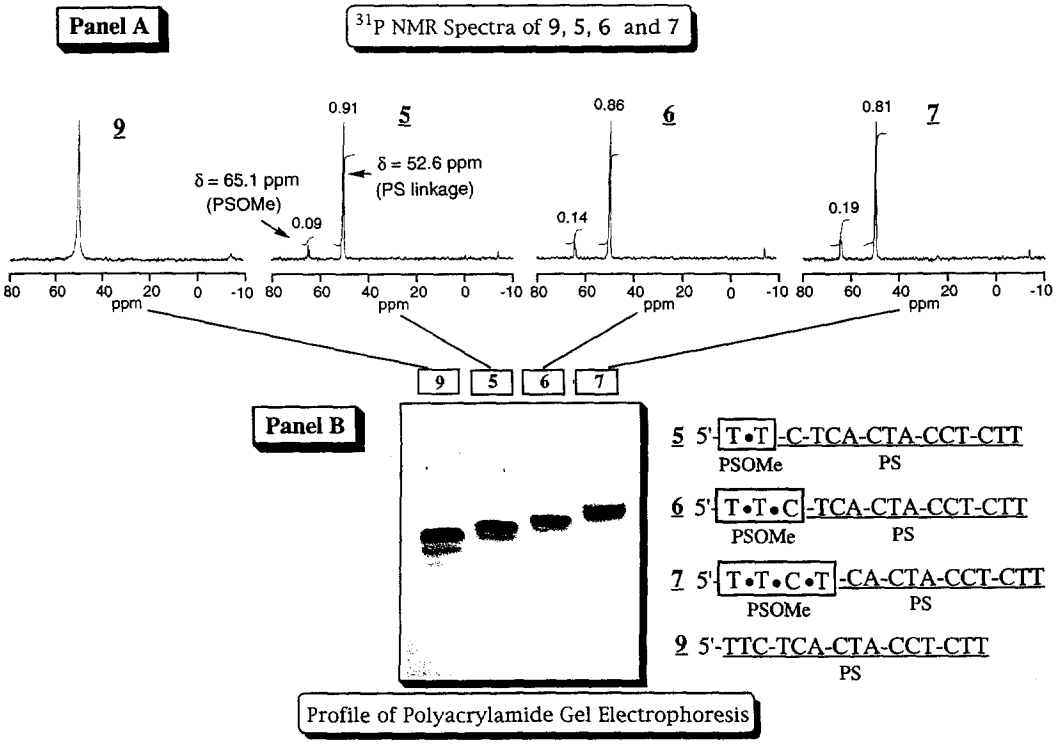

Fig. 6. ^{31}P NMR (**Panel A**) and PAGE (**Panel B**) profiles of MBOs **5-7** and the parent oligonucleotide **9**.

The helix-to-coil transitions of the duplexes formed between MBOs and the corresponding complementary 15-mer DNA strand were determined by measurements of the absorbance at λ_{260} nm vs. temperature. All complexes showed a monophasic melting transition which is characteristic of oligonucleotides. The T_ms (which depict the average of at least two determinations in each case) are revealed in Table 1. These trends in the T_ms are noteworthy: (a) The replacement of one PO linkage at the 5' ends in the PO oligonucleotide **23** by one linkage (MBO **10**) caused no change in the T_m where as the substitution with two POOMe linkages (MBO **11**) produced a marginal reduction (- 0.7 °C) in the T_m as compared to the parent **23**, (b) The replacement of PS linkages at the 5'- ends in the PS oligonucleotide **24** by one POOMe linkage (**12**) resulted in a marginal increase in the T_m (~ + 0.4 °C), whereas the substitution by two linkages (**13**) resulted in a slight decrease (~ - 0.7 °C) as compared to the parent **24**, (c) The replacement of the PS linkages at the 3'-ends of **24** by one POOMe linkage resulted in almost no change in the T_m (~ + 0.2 °C), whereas the substitution by two linkages resulted in a slight drop (~ - 0.7 °C), (d) The substitution of one PS linkage at each of the 3'- and 5'-ends by POOMe linkage (**16**) resulted in a marginal increase in the T_m (~ + 0.5 °C) and, (e) Similar trends were observed when PSOMe linkages were substituted for the PS linkages, although the gain or drop in the T_m was slightly more pronounced (see: **17** vs. **12**, and **20** vs. **13**).

These results suggest that the duplex stabilizing/destabilizing effect, as a reflection of the T_m values of the MBOs, is dependent on these factors: (a) the nature of the ionic segment of the MBO, (b) the site of incorporation of the phosphotriester group, (c) the number of triester modifications which are incorporated, and (d) the structure of the triester group. It is to be noted that in all the 15-mer sequences employed in the present study, there is the fortuitous presence of a contiguous TT segment at the 3'- and 5'- ends. The slight gain in the T_m that is observed in the case of the analogs **12**, **14**, **16**, and **17** appears to be contingent upon and limited to the presence of the TT methylphosphotriester segment. However, the factors which contribute to this gain in the T_m are unknown at this time. Nevertheless it appears, from % hypochromicity changes (11 to 13% for MBOs **12-16** vs 14% for **24**) revealed in the absorbance vs. temperature plot (Figure 7), that there is a slight decrease

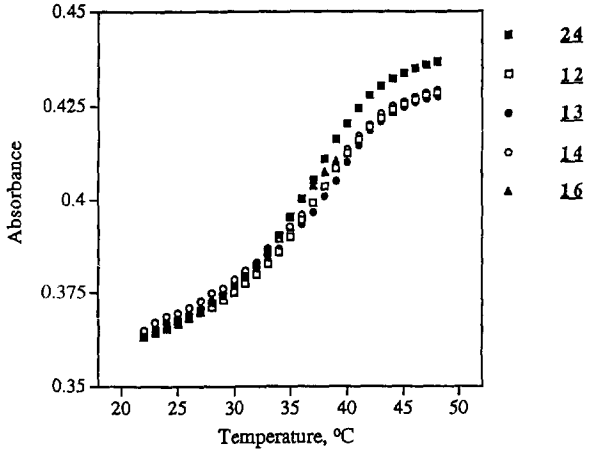

Fig. 7. Plots of absorbance (A_{260}) vs. temperature melting curves of the duplexes formed between selected MBOs (**12, 13, 14, 16**), the "all PS" analog **24**, and the complementary DNA.

Table 1. Comparative T_m Data of MBOs 10-22 (against complementary DNA).

Seq. #	Sequence	T_m °C	ΔT_m
23	5' TTC-TCA-CTA-CCT-CTT (PO)	47.8	—
10	5' [T•T] (POOMe) -C-TCA-CTA-CCT-CTT (PO)	47.8	—
11	5' [T•T•C] (POOMe) -TCA-CTA-CCT-CTT (PO)	47.1	-0.7
24	5' TTC-TCA-CTA-CCT-CTT (PS)	36.9	—
12	5' [T•T] (POOMe) -C-TCA-CTA-CCT-CTT (PS)	37.3	+0.4
13	5' [T•T•C] (POOMe) -TCA-CTA-CCT-CTT (PS)	36.2	-0.7
14	5' TTC-TCA-CTA-CCT-C- [T•T] (PS / POOMe)	37.1	+0.2
15	5' TTC-TCA-CTA-CCT- [C•T•T] (PS / POOMe)	36.2	-0.7
16	5' [T•T] (POOMe) - C-TCA-CTA-CCT-C- [T•T] (PS / POOMe)	37.4	+0.5
17	5' [T•T] (PSOMe) - C-TCA-CTA-CCT-CTT (PS)	36.5	-0.4
18	5' [T•T•C] (PSOMe) -TCA-CTA-CCT-CTT (PS)	34.9	-2.0
19	5' TTC-TCA-CTA-CCT-C - [T•T] (PS / PSOMe)	35.7	-1.2
20	5' TTC-TCA-CTA-CCT- [C•T•T] (PS / PSOMe)	33.7	-3.2
21	5' [T•T] (PSOMe) - C-TCA-CTA-CCT-C- [T•T] (PS / PSOMe)	36.1	-0.8
22	5' TTC-TCA- [C•T•A] (PS / PSOMe / PS) -CCT-CTT	34.4	-2.5

All T_ms represent the average of at least two determinations.

in the stacking of the bases in the MBOs incorporating methylphosphotriester linkages as the non-ionic segment. Based on the measurements of the ε_{max} of dinucleoside triesters, it has been previously suggested[1] that there is less base stacking in the dinucleoside triesters in solution compared to the corresponding diesters.

Overall, our studies reveal that, in most cases, the incorporation of the triester segment in an oligonucleotide sequence, only marginally affects the T_m values depending on the sequence, and the site of incorporation, while at the same time allowing for cooperativity during the thermal denaturation process. However, there appears to be no significant increase in stability due to decreased repulsion between the negatively charged phosphate of the complementary partner and the MBOs which have small segments of the neutral phosphotriester backbone.

The above results were corroborated in studies using selected antisense oligonucleotide sequences of longer length. For this purpose, we initially chose to make analogs of GEM 91® (**25**) a 25-mer "all PS" oligonucleotide sequence targeted against the *gag* mRNA of HIV-1.[13] The MBO analogs **26-32** (Table 2) of

Table 2. Comparative T_m Data of GEM 91® Analogs 25-32.

Seq. #	Sequence	T_m (°C)¶	T_m (°C)§
25	5' CTC-TCG-CAC-CCA-TCT-CTC-TCC-TTC-T (PS)	54.0	64.2
26	5' C•T•C (PSOMe) -TCG-CAC-CCA-TCT-CTC-TCC-TTC-T (PS)	52.5	62.5
27	5' C•T•C•T (PSOMe) -CG-CAC-CCA-TCT-CTC-TCC-TTC-T (PS)	51.5	61.8
28	5' C•T•C•T•C (PSOMe) -G-CAC-CCA-TCT-CTC-TCC-TTC-T (PS)	50.7	60.6
29	5' CTC-TCG-CAC-CCA-TCT-CTC-TCC-T- T•C•T (PSOMe) (PS)	51.0	62.0
30	5' CTC-TCG-CAC-CCA-TCT-CTC-TCC- T•T•C•T (PSOMe) (PS)	50.3	61.1
31	5' C•T•C (PSOMe) -TCG-CAC-CCA-TCT-CTC-TCC-T- T•C•T (PSOMe) (PS)	49.1	60.5
32	5' CTC-TCG-CAC-CCA- T•C•T•C (PSOMe) -TCT-CCT-TCT (PS) (PS)	50.8	60.3

¶ Against complementary DNA (30-mer) (PO); § Against complementary RNA (25-mer) (PO); All T_ms represent the average of at least two determinations.

GEM 91®, having PSOMe and PS linkages, and encompassing the oligonucleotide designs shown in Figure 1, were prepared and characterized by ^{31}P NMR and PAGE as detailed before. Additional structure proof was obtained by the conversion of selected analogs from among **26-32** to the parent **25** following demethylation

with 2-mercaptobenzothiazole (data not shown). The T_m values of **25-32** (Table 2) were determined using complementary 30-mer DNA (**33**) and 25-mer RNA (**34**) sequences. The absorbance vs. temperature profiles, when RNA is used as the complementary strand, are shown in Figure 8. Both from Table 2 and Figure 8, it is

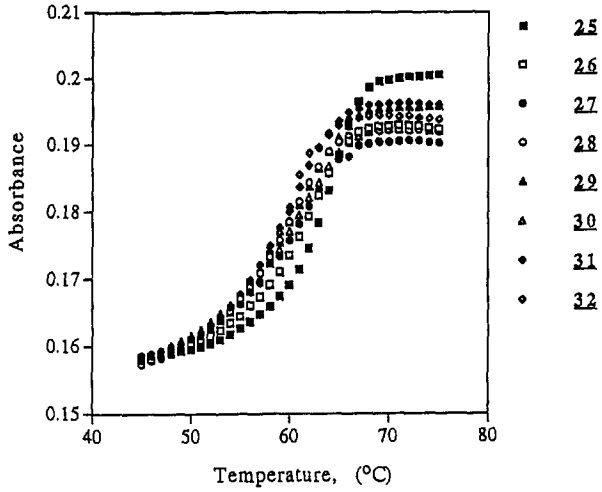

Fig. 8. Plots of absorbance (A_{260}) vs. temperature melting curves of the duplexes formed between MBOs (**25-32**), and the "all PS" analog **25**, with complementary RNA.

clear that in the case of GEM 91® analogs, the incorporation of the triester segment only marginally affects the T_m values depending on the number of PSOMe linkages and their site of incorporation in the MBO. However, in the case of the MBOs **26-32**, there was no significant increase in stability of the duplexes resulting from decreased repulsion between the negatively charged phosphate of the complementary partner and the MBOs which have small segments of the phosphotriester backbone.

Nuclease stability of MBOs

As outlined earlier, one of the objectives in designing the antisense MBOs was to develop more nuclease-resistant oligonucleotides, while at the same time, essentially preserving the other desirable attributes for the antisense activity. To ascertain this, a comparative *in vitro* evaluation of the nuclease stability of the selectd analogs **25-32** was undertaken. Thus, the oligonucleotides were 5'-end labeled using [γ-^{32}P]ATP in the presence of *polynucleotide kinase*. The 5'-^{32}P-labeled MBOs, **26-28** and **29-32**, were then incubated with *snake venom phosphodiesterase (SVPD)*. To enable comparative evaluation of their stability in each case, the ratio of the units of enzyme activity/A_{260} of the oligonucleotide employed, as well as, the assay conditions chosen were such that there was a noticeable degradation of the standard "all PS" analog GEM 91® (**25**) within 1 h following incubation. For the assay, the aliquots were drawn at different time points, and subjected to PAGE followed by autoradiography. As shown in Figure 9 (which shows a representative PAGE profile at 30 min time point), the MBOs, **29** and **30** (Figure 9, Panel B) were relatively more resistant to degradation compared to **25** (Figure 9, Panel B), when exposed to the *SVPD*, which has 3'-exonuclease activity. Thus e.g., whereas in the case of **25**, there was a ladder of fragments indicative of nuclease digestion, the digestion profiles of

MBOs **29** and **30** were marked by the presence of mostly "intact" material. The presence of the faint ladder of fragments could suggest that either: (a) the nuclease can "skip" the short 3'-triester tract in the MBO, and start to degrade the PS segment as has been observed with other 3'-capped oligonucleotides[3b] or (b) the presence of trace amounts of demethylated products either generated during the enzymatic digestion in Tris buffer at pH 8.5 or originally present in the MBO sample which then became susceptible to further nucleolytic degradation.

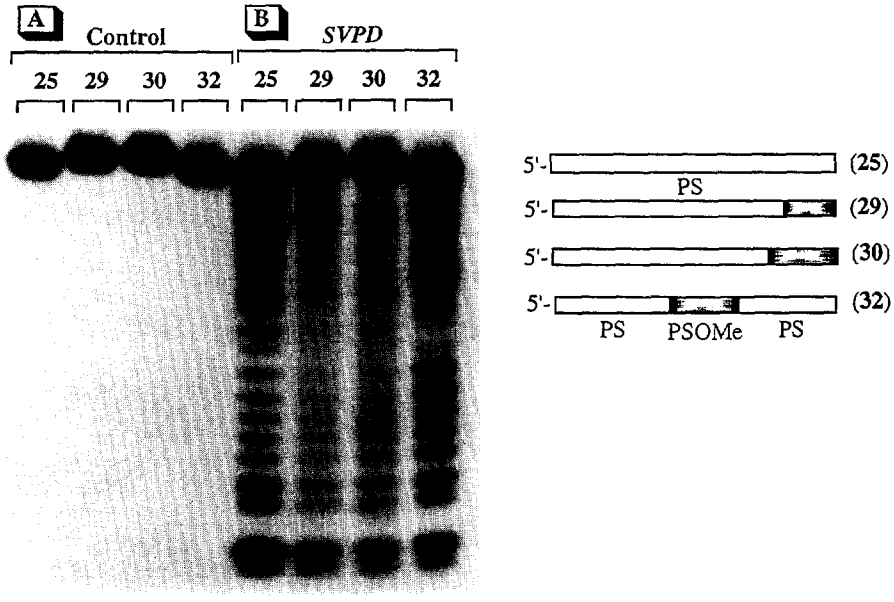

Fig. 9. Autoradiographic profiles of 5'[^{32}P]-labeled MBOs **29**, **30**, **32** and the "all PS" analog **25** after 30 min treament with *snake venom phosphodiesterase*. **Panel A,** control; **Panel B,** after treatment with *SVPD*.

In the case of the "inverted" MBO **32**, the digestion proceeded until the triester segment was reached, after which, further digestion seemed to have slowed down as indicated by the presence of a distinct 16-mer fragment.

The nuclease stability of the 5'-MBOs **26-28**, was evaluated against *SVPD*, and also against *DNA polymerase I (Pol 1)* and human serum. As shown in Figure 10, the MBOs **26-28** were relatively more resistant to degradation compared to **25** when exposed to the *3'-exonuclease SVPD* and *E.Coli Pol 1* which has 3'- as well as 5'-exonuclease activity. Apparently, although both *SVPD* and *Pol I* are 3'-exonucleases, the incorporation of phosphotriester segments at the 5'-ends seems to confer some degree of resistance to the action of these nucleases. In the case of human serum, following their incubation for 12 h, all the analogs appeared to

be intact. Thus, it appears that the incorporation of the phosphotriester segment in an MBO increases the stability against nuclease-mediated degradation compared to the parent oligonucleotide.

In conclusion, our studies using MBOs containing the non-ionic methylphosphotriester linkages demonstrate the benefits of oligonucleotide design, in conjunction with the appropriate choice of the non-ionic linkage, in modulating the antisense properties of an oligonucleotide. The synthesis of these MBOs with methylphosphotriester oligonucleotide segments can be routinely performed using *PNT* nucleoside phosphoramidite monomers. Additionally, in conjunction with *PNT* nucleoside H-phosphonate monomers, MBOs incorporating other novel non-ionic linkages have been prepared. The evaluation of biological activity of specific antisense MBOs against target m-RNAs, using both *in vitro* and *in vivo* models, are under way. The pharmacokinetics of the MBOs using radiolabeled oligonucleotides are also in progress and will be reported in due course.

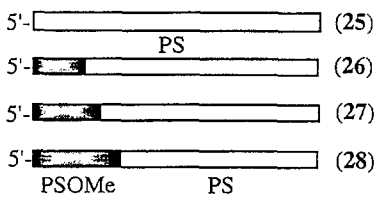

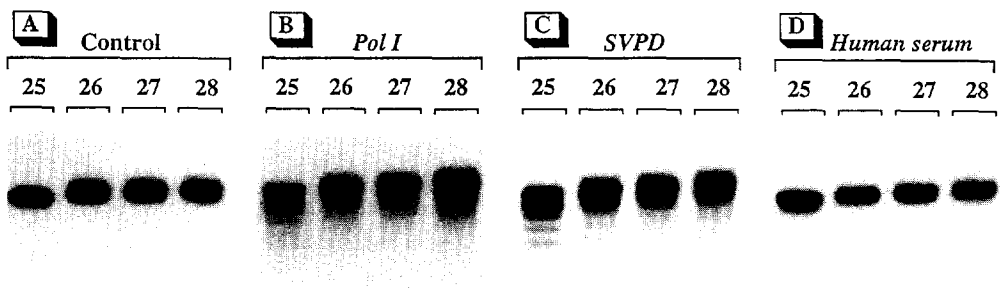

Fig. 10. Autoradiographic profiles of 5'[^{32}P]-labeled MBOs **26-28**, and the "all PS" analog **25** following 30 min treatment with different nucleases. **Panel A**, control; **Panel B**, with *DNA polymerase I;* **Panel C**, with *snake venom phosphodiesterase*; **Panel D** with human serum.

EXPERIMENTAL SECTION

Chemicals and high purity/anhydrous solvents were purchased from commercial vendors and used without further purification. Routine custom synthesis (40 to 50 g scale) of 5'-*O*-DMT *PNT* nucleoside phosphoramidite monomers (*MEPNT* and *CEPNT*) was carried out by Prime Organics, Lowell, MA, as per published protocols. CPG, derivatized with the *PNT* nucleosides, was prepared using standard protocols.[8]

Snake venom phosphodiesterase (Boehringer and Mannheim) and *alkaline phosphatase* (Pharmacia) were purchased and used as recommended by the manufacturer.

Electrophoretic analysis (PAGE) was carried out on 10 to 20% polyacrylamide-7M urea gels using electrophoresis purity reagents (National Diagnostics, Atlanta, GA). TBE was employed as the running buffer and PAGE was carried out in an assembly equipped for water circulation. Upon exposure to UV light (λ_{254} nm) and visualization against a fluorescent background (silica gel F_{254} TLC plate), the oligonucleotides were seen as dark bands.

Analytical reversed-phase HPLC (Waters 600E instrument equipped with a 996 Photodiode Array UV detector) was done using a 8NV C-18 4 μm Radial Pak cartridge column, a gradient of 100% A to 60% B over 70 min of buffer A (0.1 M NH_4OAc) and buffer B (80/20, CH_3CN/0.1 M NH_4OAc), and a flow rate of 1.5 mL/min. Preparative HPLC was performed as described before.[14]

^{31}P NMR spectra were recorded in D_2O (85% H_3PO_4 as the external reference, δ = 0) using a Varian 300 spectrometer operating in the presence of broad-band decoupling at 7.05 Tesla. MALDI-TOF mass spectral measurements were performed by The Midland Certified Reagent Company, Midland, Texas.

Solid-phase syntheses of oligonucleotides were done using a BIOSEARCH 8700 DNA synthesizer or EXPEDITE synthesizer (PerSeptive Biosystems) and used as recommended by the manufacturer. For a representative synthesis cycle, see Scheme 1 and Table 3. Solutions of the *PNT* phosphoramidites in acetonitrile (0.08 M), and 1*H*-tetrazole (0.5 M) as activator were employed. The capping step was done using two reagents CAP A (AC_2O/2,6 lutidine/THF, 1/1/8) and CAP B (N-methylimidazole solution in THF, 16% *w/v*). The solid-phase synthesis was carried out on controlled-pore-glass (CPG) (500 Å) solid support. Oxidation of the internucleotidic phosphite linkage was carried out using *tert*-butyl hydroperoxide (1 M in toluene) over a period of 1 min. The oxidative sulfurization reaction was effected by a 2% solution of the crystalline 3*H*-benzodithiol-3-one-1,1-dioxide (R. I. Chemical., Costa Mesa, CA) in acetonitrile (Burdick & Jackson, 0.01% water). The sulfurization reaction was performed over a period of 45 s - 2 min depending on the scale of synthesis. Oligonucleotides were handled using sterile gloves, eppendorf tubes and sterile disposable pipet tips.

Preparation of CPG-bound dC^{PNT}, dA^{PNT} and dG^{PNT} nucleosides

These were carried out according to standard protocols. Typical nucleoside loadings were 40-60 μmol/g.

Synthesis of the MBOs

The MBOs were synthesized on 1 to 10 μmol scale according to Scheme 1 and employing the synthesis cycle in Table 1. Following their synthesis, the CPG was subjected to either protocol A, I_2 (2% in pyridine/MeOH, 98/2, 30 min), washed with CH_3CN, and treated with K_2CO_3/MeOH (0.05 M, rt, 18 h) or protocol B,

K_2CO_3/MeOH (0.05 M, rt, 24-36 h). The CPG suspension was carefully neutralized with glacial acetic acid (ca. 5 μL). After centrifugation, the supernatant was collected. CPG was resuspended in H_2O (500 μL) and filtered.

Table 3. Synthesis Cycle for oligonucleotide synthesis (1 μmol scale).

Step	Reagent/solvent	Function	Time (sec)	Quantity of reagent delivered (mL)
1.	3% TCA/DCM	Detritylation	50	0.75
2.	CH_3CN	Wash	20	0.82
3.	0.08 M phosphoramidite/tetrazole	coupling	45	0.22
4.	CH_3CN	wash	56	0.50
5.	*tert*-BuOOH (1 M in toluene)	oxidation	60	0.50
	or			
	3*H*-BD (2% in CH_3CN)	sulfurization	8	0.30
6.	CH_3CN	wash	98	1.50
7.	Cap A, Cap B	capping	15	0.30
8.	CH_3CN	wash	98	1.50

TCA = trichloroacetic acid; DCM = dichloromethane; 3*H*-BD = 3*H*-benzodithiole-3-one-1,1 dioxide; CAP A contains acetic anhydride and 2,6-lutidine in THF; CAP B contains N-methyl imidazole in THF.

The filtrate, as well as, the supernatant were combined, and the solvent removed using a speed vac to give ca. 40 A_{260} units (1 μmol scale) or 350 A_{260} units (10 μmol) of the crude oligonucleotide. The crude oligonucleotides were purified by preparative HPLC, detritylated, and processed as described before,[14] to yield ca. 30 (1 μmol scale) and 200 (10 μmol scale) A_{260} units respectively of the purified oligonucleotides.

Base Composition analysis. MBOs 3 and 4 (Figure 2)

To approximately 1.5 A_{260} units of the MBO in 15 μL sterile water was added Tris.HCl buffer (250 mM, pH 9.0, 100 μL) and 0.015 units of *snake venom phosphodiesterase*. The mixture was incubated for 3 h at 37 °C. To the above incubate was added 10 μL $MgCl_2$ (0.5 M), alkaline phosphatase (2 μL, 4 units), and incubated at 37 °C for 12 h. The reaction mixture was analyzed by reversed-phase HPLC using 8NV C_{18} 4 μm Radial Pak Cartridge Column using a gradient of 100% A to 60% B over 70 minutes at a flow rate of 1.5 mL/min (solvent A: 0.1 M NH_4OAc; solvent B: CH_3CN/solvent A, 80/20). The elution order of the nucleosides under these conditions was dC, dG, T and dA.

Thermal denaturation studies

These studies on MBOs were carried out using sense DNA and sense RNA. For each determination a mixture of the sense oligonucleotide and the MBO (0.2 A_{260} units of each) in 1 mL of buffer (100 mM NaCl, 10 mM NaH_2PO_4, pH 7.4) were heated to 95 °C for 5 min and gradually cooled to room temperature. The samples were heated at the rate of 0.5 °C/min prior to the measurements of absorbance. Thermal transitions in absorbance were recorded at λ_{260} nm using a GBC 920 double beam UV/Visible spectrophotometer.

Nuclease-stability studies

(a) ***^{32}P-labeling.*** The oligonucleotides were ^{32}P-labeled at the 5'-end using [γ-^{32}P]ATP. Typically, to ca. 10 ng of the MBO in 1 μL of sterile water, was added 10 units of *polynucleotide kinase* (New England Biolabs), 1 μL of 10 X kinase buffer, 0.01 mCi of [γ^{32}P-ATP] (6 Ci/mmol, Amersham) and sterile water q.s. to a total volume of 10 μL. The mixture was incubated at 37 °C for one hour and purified by PAGE.

(b) Stability studies with human serum. Dried samples of the ^{32}P-labeled MBOs (5 X 10^5 cpm) were incubated at ambient temperature with 20 μL of human serum each. The incubate was treated with DNA extraction buffer (3 μL), proteinase K (1 μL, 10 mg/mL). After 1 h at 37 °C, the protein was extracted by addition of equal volume of phenol, followed by chloroform. To the resulting digest, formamide (3 μL) was added and the samples subjected to PAGE (20%, 8 M urea) followed by autoradiography.

(c) Stability studies with DNA polymerase I. To samples of the ^{32}P-labeled MBOs (5 X 10^5 cpm) was sequentially added, DNA polymerase buffer (10X, 2 μL), *DNA polymerase I* (20 units, *E. Coli*-derived) (Worthington Biochemicals), H_2O (20 μL), and incubated at 37 °C for 1 h. Then, EDTA (1 μL, 0.5 M, pH 8.0) followed by formamide (3 μL) was added, and the samples subjected to PAGE (20%, 8 M urea) followed by autoradiography.

(d) Stability studies with snake venom phosphodiesterase. To samples of the ^{32}P-labeled MBOs (5 X 10^5 cpm) was added Tris.HCl buffer (2 μL, 250 mM, pH 9.2), phosphodiesterase (2 μL, 1 mg protein/0.5 mL), and water (20 μL). After incubation at 37 °C for 1 h, formamide (3 μL) was added and the samples subjected to PAGE (20%, 8 M urea) followed by autoradiography.

Acknowledgement: We thank the referees for their comments and suggestions.

REFERENCES AND NOTES

1. Miller, P. S.; Fang, K. N.; Kondo, N. S.; Ts'o, P. O. P. *J. Am. Chem. Soc.* **1971**, *93*, 6657-65.
2. (a) Liu, A. -L.; Jack, W. E.; Modrich, P. *J. Biol. Chem.* **1981**, *256*, 13200; (b) Weinfeld, M.; Livingston, D. C. *Biochemistry* **1986**, *25*, 5083.
3. For selected reviews see: (a) Uhlmann, E.; Peyman, A. *Chem. Rev.* **1990**, *90*, 544-84; (b) Agrawal, S.; Iyer, R. P. *Curr. Op. Biotech.* **1995**, *6*, 12-19 and references therein; (c) Thuong, N. T.; Helene, C. *Angew. Chem. Intl. Ed. Engl.* **1993**, *32*, 666-690.

4. Zhang, R.; Iyer, R. P.; Tan, W.; Yu, D.; Zhang, X.; Lu, Z.; Zhao, H.; Agrawal, S. *J. Pharmacol. Exp. Therap.* **1996,** *278,* 971-79.
5. (a) Furdon, P.; Dominski, Z.; Kole, R. *Nucl. Acids Res.* **1989,** *17,* 9193; (b) Agrawal, S.; Mayrand, S. H.; Zamecnik, P. C.; Pederson, T. *Proc. Natl. Acad. Sci. (USA)* **1990,** *87,* 1401-4.
6. (a) Koole, L. H.; van Genderen, M. H. P.; Buck, H. M. *J. Am. Chem. Soc.* **1987,** *109,* 3916-21; (b) van Genderen, M. H. P.; Koole, L. H.; Aagaard, O. M.; van Lare, C. E. J.; Buck, H. M. *Biopolymers,* **1987,** *26,* 1447-61.
7. Miller, P. S.; Dreon, N.; Pulford, S. M.; McParland, K. M. *J. Biol. Chem.* **1980,** *255,* 9659-9665.
8. (a) Iyer, R. P.; Yu, D.; Ho, N.-H.; Devlin, T.; Agrawal, S. *J. Org. Chem.* **1995,** *60,* 8132-33; (b) Yu, D.; Iyer, R. P.; Ho, N.-H.; Devlin, T.; Agrawal, S. (submitted); (c) During model studies of deprotection of dG^{PNT} (but not with dC or dA) using I_2/pyridine/H_2O, small amounts of an intermediate addition product (see structure below) was observed which underwent conversion to dG upon K_2CO_3/MeOH treatment. Although, the formation of this adduct was of no consequence in the deprotection using I_2/pyridine/H_2O followed by K_2CO_3/MeOH treatment, it could be avoided by conducting the deprotection using a 2% solution of iodine in pyridine/MeOH, 98/2. For the present study, the G-rich oligonucleotide was intentionally chosen to demonstrate that complete deprotection of dG^{PNT} was accomplished using this protocol.

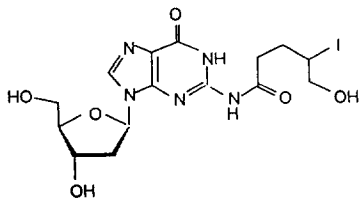

9. (a) Vinogradov, S.; Asseline, U.; Thuong, N. T. *Tetrahedron Lett.* **1993,** *34,* 5899-5902; (b) Hayakawa, Y.; Hirose, M.; Hayakawa, M.; Noyori, R. *J. Org. Chem.* **1995,** *60,* 925-30; (c) Alul, R. H.; Singman, C. N.; Zhang, G.; Letsinger, R. L. *Nucl. Acids Res.* **1991,** *19,* 1527-32; (d) Kuijpers, W. H. A.; Huskens, J.; Koole, L. H.; van Boeckel, C. A. A. *Nucl. Acids Res.* **1990,** *18,* 5197-5205; (e) Koole, L. H.; Moody, M. H.; Broeders, N. L. H. L.; Quaedflieg, P. L. J. M.; Kuijpers, W. H. A.; van Genderen, M. H. P.; Coenen, A. J. J. M.; van der Wal, S.; Buck, H. M. *J. Org. Chem.* **1989,** *54,* 1657-64.
10. (a) Beaucage, S. L.; Caruthers, M. H. *Tetrahedron Lett.* **1981,** *22,* 1859-62; For reviews see: (i) Beaucage, S. L.; Iyer, R. P. *Tetrahedron* **1992,** *48,* 2223-2311; (ii) Beaucage, S. L. in *Protocols for Oligonucleotides and Analogs*; Agrawal, S., Ed.; Humana Press: Totowa, NJ, 1993; Vol. 20, pp. 33-61.
11. Iyer, R. P.; Egan, W.; Regan, J. B.; Beaucage, S. L. *J. Am. Chem. Soc.* **1990,** *112,* 1253-54.
12. For selected examples see: (a) De Mesmaeker, A.; Lebreton, J.; Waldner, A.; Fritsch, V.; Wolf, R. M. *Bioorg. Med. Chem. Lett.* **1994,** *4,* 873-78; (b) Caulfield, T. J.; Prasad, C. V. C.; Prouty, C. P.; Saha, A. K.; Sardaro, M. P.; Schairer, W. C.; Yawman, A.; Upson, D. A.; Kruse, L. I. *Bioorg. Med. Chem. Lett.* **1993,** *3,* 2771-76; (c) Kutterer, K. M. K.; Just, G. *Bioorg. Med. Chem. Lett.* **1994,** *4,* 435-38; (d) Bevierre, M.-O.; De Mesmaeker, A.; Wolf, R. M.; Freier, S. *Bioorg. Med. Chem. Lett.* **1994,** *4,* 237-240. For additional examples see Ref. 3b.
13. Agrawal, S.; Iyer, R. P. *Drugs of the Future* **1995,** *20,* 344-351.
14. For details, see: Iyer, R. P.; Yu, D.; Agrawal, S. *Bioorg. Chem.* **1995,** *23,* 1-21.

(*Received in USA* 10 *July* 1996; *revised* 16 *August* 1996; *accepted* 23 *September* 1996)